

# ON DESIGNING IMPEDANCE TUBE WITH GRAZING FLOW

<sup>a)</sup>Vadim Palchikovskiy, <sup>a)</sup>Igor Khramtsov, <sup>a)</sup>Aleksander Kuznetsov, <sup>a)</sup>Victor Pavlogradskiy

<sup>a)</sup>Perm National Research Polytechnic University (PNRPU), Perm, Russia, lmgsh@pstu.ru

**Abstract:** The article considers the general issues arising in designing the experimental setup “Impedance tube with grazing flow”, the main structural units of the setup, and their purpose. It is given the basic requirements to be provided by the setup when testing samples of acoustic liners used in an aircraft engine. The choosing of the design parameters of the setup is based on the analysis of the known analytical solutions of the acoustics and gas dynamics, and on the numerical simulation of the grazing flow in the impedance tube.

**Keywords:** impedance tube with grazing flow, acoustic liner, multichannel measurements, impedance, numerical simulation, flow velocity profile

**DOI:** 10.36336/akustika20213980

## 1. INTRODUCTION

The verification of the impedance of the acoustic liner developed for the aircraft engine to their design values is carried out on a special setup called “Impedance tube with grazing flow” (ITGF). The setup is a narrow tube, usually of rectangular or square cross-section, which is due to the simplicity of manufacturing the liner sample and the convenience of its mounting on the duct walls. Sound and flow are simultaneously passed through the duct. The waves propagating from the acoustic drivers are attenuated as they pass through the anechoic terminations.

The narrowness of the duct is caused by the possibility of generating a flow with the required speed at a low mass flow rate. In this case, the use of high-power units for air supply is not required. It also allows for high sound pressure levels (SPL) to be generated in the duct by a few acoustic drivers. Achieving high flow rates and high SPL are important requirements when testing liner samples on the ITGF setup, as these conditions are equivalent to the operating conditions of the full-scale acoustic liners in aircraft engine. At the same time, the fact that the sound field structure in a rather narrow tube does not correspond to the sound field structure in the real duct of the aircraft engine is not fundamental, since the locally reacting liners are of the greatest practical interest. The impedance of such liners does not depend on the sound field structure, but it is determined by the design features of the liner and the aeroacoustic parameters near the duct wall (grazing flow velocity, the thickness of the boundary layer, the frequency spectrum of the noise source, etc.).

An array of microphones intended to measure the acoustic pressure along the duct is mounted on the setup wall opposite the liner sample. The acoustic pressure obtained in the experiment is processed by various computational procedures to determine the impedance of the tested sample. The narrow duct also ensures only plane wave propagation in the rigid-walled sections of the setup over the frequency range of interest, which is very convenient to set the boundary conditions in the computational procedures.

Investigations on such setups were begun in the last century [1, 2]. At present, the setups exist in various scientific centers of the world dealing with the issues of reducing aircraft noise [3-15]. The structure and operation principles of these setups are the same as above. A basic scheme of the ITGF setup is shown in Fig. 1.

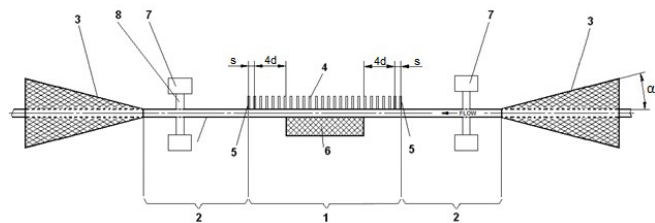


Fig. 1: A basic scheme of the ITGF setup

According to the scheme, the setup can be broadly divided into a test section (pos. 1), a section of acoustic drivers (pos. 2) and a section of anechoic terminations (pos. 3). The test section consists of the microphones (pos. 4, 5) and liner sample holder (pos. 6). Since acoustic liners in an aircraft engine operate under conditions of sound propagation both downstream (for example, in the bypass duct) and upstream (air intake duct), similar conditions should be provided when testing samples. Therefore, the setup can be equipped with two sections of acoustic drivers (pos. 7). In order to place several acoustic drivers in one section of a duct, they should not interfere with each other. For this, the acoustic drivers are placed at a certain distance from the setup walls and are attached to the setup through the narrow tubes (pos. 8). Anechoic terminations (pos. 3) are necessary to reduce the amplitudes of sound waves reflected from the exit sections of the setup back into the duct, where they interfere with direct incident sound waves and, accordingly, make an unnecessary contribution to the signals measured by the microphones.

The following are some basic assumptions that can be used to select design parameters of the setup "Impedance tube with grazing flow".

## 2. DESIGNING BASED ON ACOUSTICAL PRINCIPLES

For the ITGF setup with a rectangular duct cross section, the sound field in the presence of a flow is described by the Helmholtz convective equation in Cartesian coordinates:

$$(1 - M_0^2) \frac{\partial^2 p}{\partial z^2} - 2ikM_0 \frac{\partial p}{\partial z} + \frac{\partial^2 p}{\partial x^2} + \frac{\partial^2 p}{\partial y^2} + k^2 p = 0 \quad (1)$$

where

- $p$  is an acoustic pressure;
- $M_0$  is an average Mach number;
- $k$  is a spatial wavenumber;
- $f$  is a frequency;
- $i$  is an imaginary unit;
- $z, x, y$  are the axial, vertical and spanwise locations, respectively (Fig. 2).

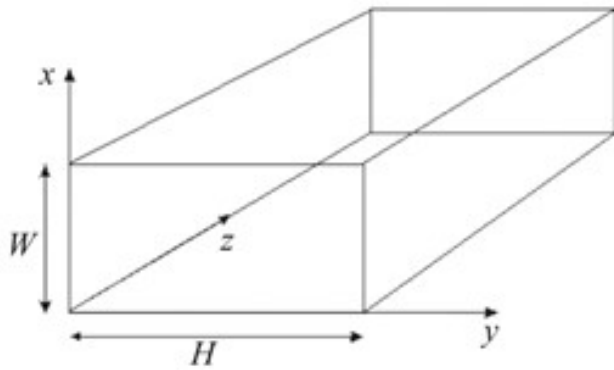


Fig. 2: Coordinate axis in rectangular duct

The solution to equation (1) for a duct with rigid walls can be written as:

$$p(x, y, z) = \sum_{m=0}^M \sum_{n=0}^N (A_{mn} e^{ik_{zmn}z} + B_{mn} e^{-ik_{zmn}z}) \cos(k_{xm}x) \cos(k_{yn}y) \quad (2)$$

where

- $M, N$  are the numbers of the transverse modes taken into account in the solution;
- $m, n$  are the counts of transverse modes;
- $A_{mn}, B_{mn}$  are the amplitude coefficients of the incident and reflected modes.

The wavenumbers of transverse modes in expression (2) are determined by the formulas

$$k_{xm} = \frac{m\pi}{W}, \quad k_{yn} = \frac{n\pi}{H} \quad (3)$$

and the axial wavenumber is determined from the expression

$$k_{zmn}^{\pm} = \frac{kM_0 \mp \sqrt{k^2 - (k_{xm}^2 + k_{yn}^2)(1 - M_0^2)}}{1 - M_0^2} \quad (4)$$

Here

$W, H$  is the cross-section dimensions of a duct (Fig. 2). The signs '±' in the designation of the axial wavenumber correspond to the positive and negative directions of the sound wave propagation.

If the mode with number  $(m, n)$  has an imaginary number  $k_{mn}$ , then this mode is attenuated. To determine the frequency at which the mode begins to attenuate (cutoff frequency), you can consider the expression under the root in formula (4). Substituting (3) in (4) yields (5):

$$f_{m,n} = \frac{c_0}{2} \sqrt{(1 - M_0^2) \left[ \left(\frac{m}{W}\right)^2 + \left(\frac{n}{H}\right)^2 \right]} \quad (5)$$

Here

$c_0$  is a sound speed.

Thus, the cutoff frequency sets the upper limit of the ITGF setup operation in the frequency range. Carrying out measurements at frequencies above the cutoff frequency requires the arrangement of the microphones at the walls of the setup in both transversal directions. For example, an arrangement wherein all microphones are shifted by one-quarter of the lateral dimension relative to the axes of symmetry is shown in Fig. 3. Such microphones arrangement excludes the measurements at a node of a standing wave for transverse mode (1, 1). Failure to comply with this requirement does not allow to correctly determine the amplitude coefficients of the modes in the rigid-walled sections of the setup and, accordingly, to correctly set the boundary conditions in the impedance reduction procedure.

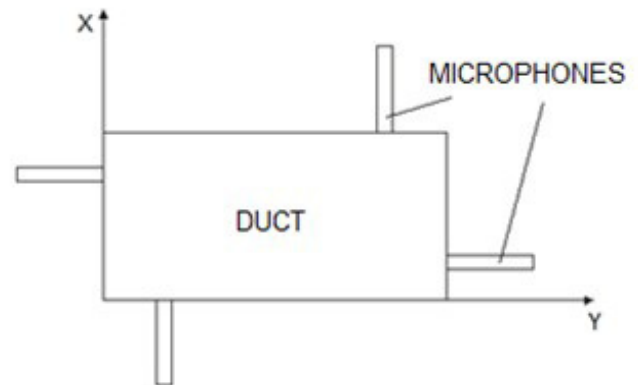


Fig. 3: Scheme of the possible arrangement of microphones in the presence of a transverse mode

In addition to the shape and dimensions of the duct, which determines the cutoff frequency, there are other design requirements for the ITGF setup, which can also significantly affect the accuracy of determining the impedance of the liner. First of all, this concerns the minimum spacing  $s$  between any two microphones used in measurements (Fig. 1). If  $s$  is equal to an integer number of half-waves, then the determinant of the system constructed from equations (2) is equal to zero [16], which prevents to find the acoustic characteristics of the liner sample at the frequency under consideration. Accordingly, the

microphones should be arranged in such a way that the frequency  $f_u$  corresponding to a half-wave equal to the spacing  $s$  is outside the frequency range of the ITGF setup (6):

$$f_u = \frac{c_0}{2s} > f_{m,n} \quad (6)$$

However, the spacing  $s$  should not be greatly reduced either. This is due to the fact that the lower limit of an ITGF frequency range (let us denote it by  $f_l$ ) is determined by the frequency, from which the change in phase of the acoustic pressure measured at two nearest points becomes noticeable. As experience demonstrates, the phase change is already ensured at a distance of 2-3% of the wavelength. Then, taking into account the spacing  $s$ , at which the phase change occurs, the value of the limiting lower frequency can be determined by the formula (7):

$$f_l = 0.025 \frac{c}{s} \quad (7)$$

Measurements on an ITGF at frequencies below  $f_l$  lead to errors in determining the acoustic impedance of the liner sample.

The entrance and exit of the test section, where the outermost microphones are located, should be selected in such a way as to the transverse modes arising at the joints of the impedance and rigid walls do not reach these microphones. For this, the distance from the edges of the liner to the entrance and exit of the test section should be at least 4-5 transverse dimensions of the duct (let us denote it by  $d$ ). The same requirement applies to the distance between the outermost microphones and the acoustic drivers sections. This is due to the fact that the presence of only plane waves on the outermost microphones significantly simplifies the setting of boundary conditions in the procedures of liner impedance education.

The length of the liner sample and, accordingly, its holder depends on the method used for determining the liner impedance and the frequency range of the setup. For example, if a single-mode method for determining impedance is used [17], then in the center of the test section it is enough to place one microphone (also at the entrance to the test section there is a reference microphone, relative to which the phase is determined). To exclude the presence of the transverse modes arising at the joints of the impedance and rigid walls on the microphone, it should be placed from the joints at a distance  $(4...5)d$ . Based on these conditions, the length of the liner sample in the single-mode method should be at least  $(8...10)d$ . There is also a popular impedance education method, based on the selection of such an impedance so that the total discrepancy between the experimental and calculated values of acoustic pressure on the microphones is minimal [17]. The method is sensitive to the absorption of sound energy in the duct (the higher the absorption, the better impedance education results). The absorption of sound energy in the duct decreases as the wavelength becomes longer than the sample. In addition, following factors affect the reduction in absorption of sound energy: a decrease in the number of layers and their depth in the liner sample, a decrease in SPL in the duct, and an increase in the flow velocity. On the other hand, a flow generates a background noise in the duct, and the noise-to-signal ratio decreases, which also negatively affects the accuracy of the impedance education. Thus, it is recommended to choose

the length of the liner sample to be equal to a wavelength at the lower frequency.

Special attention should be paid to the design of the anechoic terminations. Their principle of operation is that they gradually absorb the acoustic energy of the wave traveling to the exit section of the duct. As a result, the wave reflected from the exit section has a very small amplitude and, propagating back into the duct, passes through the anechoic terminations again, further reducing energy. If the ITGF setup has well-designed anechoic terminations, the amplitude of the reflected wave is noticeably less than of the incident wave and its contribution to the signals measured is small. The walls of the duct in a section of anechoic termination are lined with perforated sheets. The sound waves passing through the holes in perforated sheets enter the cavity with sound-absorbing material (usually fibrous materials are used) and decay there. To minimize reflections from each duct cross-section, the impedance of these cross-sections should be changed very smoothly. Therefore, the cavity height also changes smoothly along the duct, i.e. the opening angle  $\alpha$  (Fig. 1) should be small, which leads to a rather large length of the anechoic terminations.

### 3. DESIGNING BASED ON GAS-DYNAMIC PRINCIPLES

The flow in a narrow duct can be represented as a classical flow of a liquid in a pipe, which has been much studied, for example, in [18, 19]. The analytical solution for a round pipe has the form [19]:

$$\frac{U}{u_*} = 2.5 \ln \frac{u_*(r-y)}{\nu} + 5.5 \quad (8)$$

where

$U$  is a velocity at a distance  $y$  relative to the pipe axis;

$u_*$  is a local shear stress velocity;

$\nu$  is a kinematic viscosity;

$r$  is a pipe radius.

The transition from pipes with a circular cross-section to pipes of other shape is carried out using the hydraulic diameter  $d=4F/S$ ,

where

$F$  is a cross-section area;

$S$  is a wetted perimeter.

However, the analytical solution is applicable only for steady-state pipe flow. So-called *inlet length* (the distance from the initial cross-section at which the velocity profile varies) in a pipe with the laminar flow can be approximately determined by the formula [19]:

$$l_{in} = 0.03d \cdot Re \quad (9)$$

where

$Re$  is a Reynolds number. For a turbulent flow, the inlet length is much shorter than for a laminar flow and is equal to  $(50...100)d$  according to Kirsten's measurements [20], and  $(25...40)d$  according to Nikuradse's data [18]. Thus, the inlet length differs greatly, which may be associated with different initial flow conditions.

Usually, the length of the ITGF test section is  $(40 \dots 50)d$ . As a result, the liner sample is placed on the inlet length. Hence, it is necessary to take into account this variable velocity profile in the impedance education problem. However, the measurement of the velocity profile over the whole test section of the ITGF setup is a very laborious task; in addition, the presence of a measuring probe near the duct wall somewhat distorts the measurement results. In this regard, one can try to obtain a velocity profile by numerical simulation, but this requires validating the numerical model based on the results of the experiment. It is needed to consider the following factors: a flow rate, design features of the setup, surface roughness, irregularity of the velocity profile at the inlet, etc. Nevertheless, the velocity profile obtained in numerical simulation is not ideally accurate, since in a real duct there are inhomogeneities that are artificial turbulators, for example, joints between the flanges of the ITGF's units. On the other hand, if the liner sample was installed in the field of a constant velocity profile, an analytical solution could be used to describe the velocity profile.

Let us further analyze the change in the velocity profile on the basis of numerical simulation to find out where the velocity profile becomes constant. The initial configuration of the duct geometry for the numerical simulation was taken from the existing ITGF setup at the PNRPU Acoustic Research Center. The scheme of this setup is shown in Fig. 4. The base of the setup is a narrow square duct with a transverse dimension  $d=40$  mm. The length of the test section in this setup is  $51d$ . The liner sample is mounted at a distance of  $20d$  from the entrance (Fig. 4, section 0). It is possible to install liner samples with length up to  $8d$ . In sections 1 and 3, permanent Pitot tubes are installed. In section 2, it is possible to temporarily install Pitot rake to obtain a three-dimensional velocity profile.

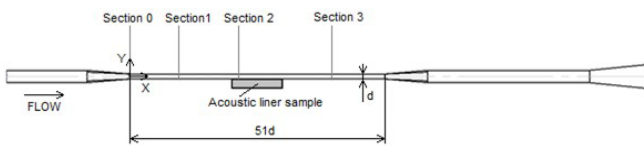


Fig. 4: Scheme of the ITGF for numerical simulation of the flow

Due to the short length of the test section ( $51d$ ), at the first stage of the numerical simulation, the length was increased to 4.5 m. The entrance to the duct remains the same as in the base model. The computational domain is shown in Fig. 5. At the entrance, the boundary condition "Inlet" was applied with a mass flow rate of 0.14749 kg/s. At the exit, the boundary condition "Outlet" with zero excess pressure was applied. On the wall, we used the "Wall" boundary condition with adhesion.

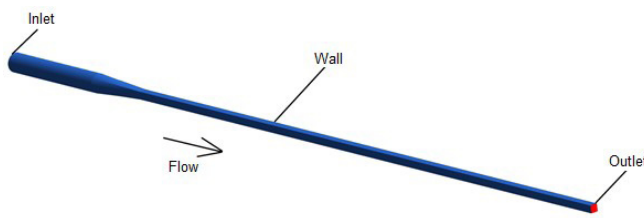


Fig. 5: Computational domain

To evaluate the influence of the computational mesh on the solution, 3 meshes were built with the following size of the element: 1.5 mm; 3 mm; 6 mm. All meshes had a thickening of elements in the wall region with a growth factor of 1.2. The

height of the first element was  $20 \mu\text{m}$ , which provided the value of the parameter  $y^+$  less than 1 for all computations. The amount of the mesh elements ranged from 0.3 to 12 million. Fig. 6 shows the mesh at the entrance in the test section of the ITGF setup.

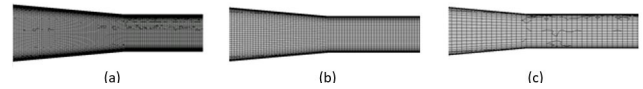


Fig. 6: Computational mesh: (a) – element size 1.5 mm, (b) – element size 3 mm, (c) – element size 6 mm

The numerical simulation was carried out in Ansys Fluent. A Steady Pressure-Based solver was used. It was applied the Shear-Stress Transport (SST)  $k-\omega$  Model, which is well suited for a wide class of flows [21]. The computations were carried out under normal atmospheric conditions and without considering the compressibility due to the low flow velocity. The computational model was verified at average flow velocity of 75 m/s, which corresponds to the Mach number  $M=0.22$ . This flow velocity is close to that in turbofan engines in a landing mode.

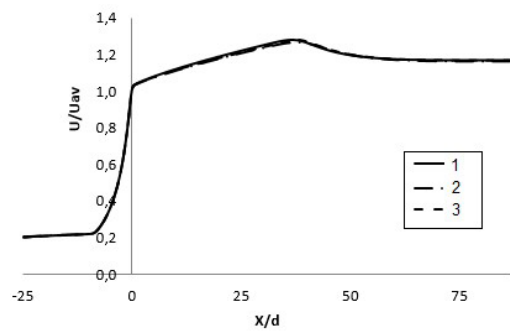


Fig. 7: Flow velocity profile in axial direction for 3 variants of computational mesh: 1 – element size 1.5 mm, 2 – element size 3 mm, 3 – element size 6 mm

To verify the obtained velocity profile it was compared with the analytical solution. Fig. 7 demonstrates the profiles of the flow velocity  $U/U_{av}$ , where  $U$  is the axial velocity taken on the duct axis,  $U_{av}$  is the axial velocity averaged in the cross-section in section 2. The section from  $-25d$  to 0 is located before the duct entrance. A narrow duct is located from 0 to  $80d$ , where all the results are considered. One can see a slight difference between the results on different meshes, which does not exceed 1%.

Additionally, the profile of a transverse velocity at a point  $75d$  was considered. At this point, the velocity profile can already be considered steady, and it gives the possibility to compare the results of numerical simulation with the analytical solution (8). Fig. 8 shows the velocity profiles at point  $75d$ . It can be seen that these profiles are weakly dependent on the mesh density (for the considered variants) and are very close to the analytical solution – the discrepancy between the results does not exceed 1%.



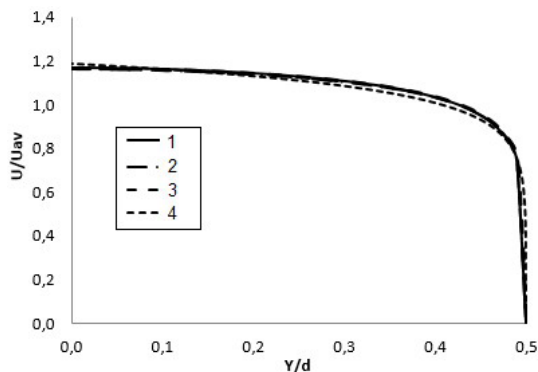


Fig. 8: Profile of a transverse velocity at point 75d: 1 – element size 1.5 mm, 2 – element size 3 mm, 3 – element size 6 mm 4 – analytical solution (8)

Based on the studies conducted, a computational mesh with element size of 3 mm was selected for further computations.

Fig. 9 shows the velocity profiles for the sections shown in Fig. 4 and for the section at point 60d. When the flow enters the channel, the velocity profile is almost uniform and the velocity on the axis is equal to  $U_{av}$ . Near the walls, the velocity increase slightly due to a change in the channel cross-section from conical to square. Near the wall, the flow velocity sharply decreases and at the wall becomes equal to 0. Along the channel, the velocity on the axis increases almost uniformly and its profile stretches due to the deceleration of the flow at the wall. At a point 37d, the collapse of the boundary layers occurs, which is accompanied by active mixing and decrease in velocity along the channel (it can be seen in Fig. 9 that the profile at point 60d has become less elongated). Starting with 60d, the velocity profile can be considered constant.

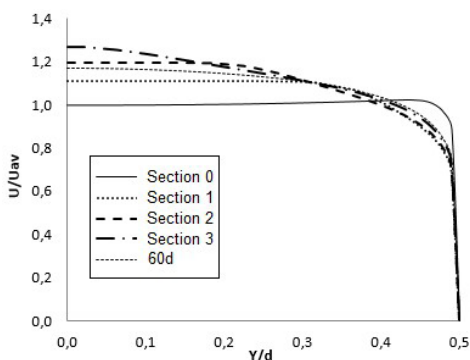


Fig. 9: Evolution of the transverse velocity profile

The effect of various factors on channel flow is discussed below. According to the formula (9), the Reynolds number should influence the inlet length. To change the Reynolds number, one can change the Mach number. It was considered the influence of the value of the average flow velocity at the entrance of the test section on the velocity profile. Additionally, the computations were carried out for velocities of 0.1 and 0.3  $M$ , at which the flow can still be considered incompressible. The results are presented in Fig. 10. It is seen that the velocity value at the entrance has little effect on the changes in the velocity profile along the channel. As the velocity increases, the profile changes more slowly along the channel length, however, the effect does not exceed  $0.5d$  and  $0.01 U_{av}$ .

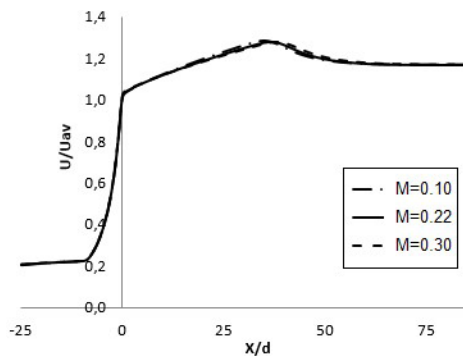


Fig. 10: Influence of the average flow velocity at the entrance of the test section on the change in the velocity profile along the channel

Various design features of the setup can also influence the velocity profile. For example, a convergence angle of the channel inlet, or the expanding channel behind the test section of the setup. The convergence angle for the existing ITGF setup is  $5\sigma$ . Additionally, computations were carried out at the convergence angle  $\beta$  (Fig. 11) equal to  $2.5^\circ$  and  $10^\circ$ . To analyze the effect of the expanding channel, it was used the design of the existing ITGF setup, the narrow channel of which has a length of  $51d$ , and then it expands. Fig. 11 shows the influence of the angle  $\beta$  on the change in velocity profile along the channel. It is seen, that this factor has no significant effect on the length of establishing a constant velocity profile.

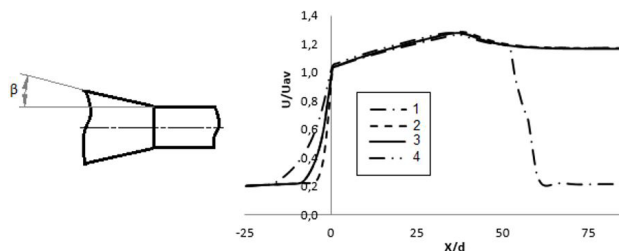


Fig. 11: Effect of the angle  $\beta$  on the velocity along the channel: 1 – existing ITGF setup, 2 –  $\beta=10^\circ$ , 3 –  $\beta=5^\circ$ , 4 –  $\beta=2.5^\circ$

In practical terms, the channel cannot be considered as a hydraulically smooth pipe. The roughness of the walls leads to the fact that the resistance is higher than when using expression (8). In this regard, flows in pipes with roughness are of great practical importance and have been the subject of numerous studies; a review of such works is presented in [22].

Generally, the sand roughness is considered. In the case of technical roughness, the resistance is usually much higher than when considering sand roughness. To convert the technical roughness to the equivalent sand roughness, it is required to know the roughness parameters of the real wall. In this work, computations are performed for relatively high values of the equivalent sand roughness, which can be close to the real roughness in the ITGF setup. Sand roughness heights  $H$  of 100, 200, and 500  $\mu\text{m}$  are considered. The results are shown in Fig. 12 and Fig. 13. As can be seen, the surface roughness leads to a much faster change in velocity in the channel. In this case, the velocity profile becomes constant faster with increasing roughness.

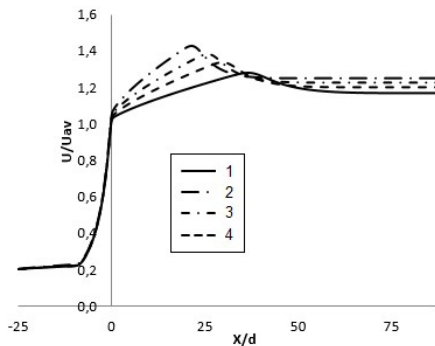


Fig. 12: Influence of roughness on the change in velocity along the channel: 1 – hydraulically smooth pipe; 2 –  $H=500 \mu\text{m}$ ; 3 –  $H=200 \mu\text{m}$ ; 4 –  $H=100 \mu\text{m}$

Fig. 13 shows the velocity profile at section 2, located in the area of the liner sample (Fig. 4). One can see that the shape of the profile changes significantly. At the same time, at the maximum of the considered roughness heights, the profile becomes constant only behind a section  $45d$ . Unfortunately, the effect of the real roughness on the velocity profile can only be determined in an experiment on the real ITGF setup. Thus, to ensure that the sample is located in the region of the constant velocity profile, the length of the test section to the sample should be increased to at least  $60d$ .

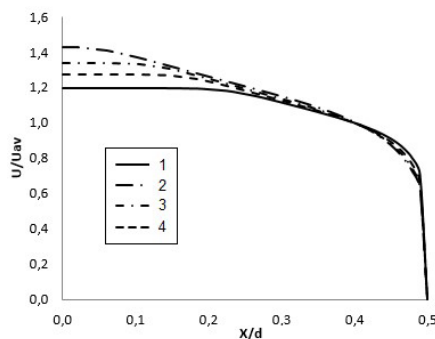


Fig. 13: Influence of roughness on velocity profile in section 2 (Fig. 4): 1 – hydraulically smooth pipe; 2 –  $H=500 \mu\text{m}$ ; 3 –  $H=200 \mu\text{m}$ ; 4 –  $H=100 \mu\text{m}$

Most of the known ITGF setups have shorter test sections to the liner sample. In part, this can be attributed to the fact that the velocity profile in the ducts of the aircraft engine has no time to become constant due to the short channels, and the samples of the developed acoustic liner must still be tested in conditions close to the conditions of real operation. However, experimentally obtaining a flow with a constant velocity profile in the ITGF's channel would be a very convenient option in the setup to conduct scientific research. For example, to verify the new models of the impedance boundary condition, where knowledge of the velocity field is required, it is convenient to use the known analytical solutions for a steady flow. In general, on the basis of the recommendations given in the article, the developers of the new impedance tubes with grazing flow, depending on the purposes of its application and the available capabilities, can choose the required test section length to the liner sample.

## 4. CONCLUSION

On the basis of the analytical solution of the Helmholtz convective equation, the main recommendations for the selection of the parameters of the impedance tube with grazing flow (ITGF) are considered. The following recommendations are given: the spacing between the microphones, the distances from the outermost microphones to the edges of the liner sample and to the acoustic driver section, the length of the liner sample depending on the method of the impedance determination.

The work also analyzes the change in the flow velocity profile along the channel and the influence of various factors on it. The analysis was carried out on the basis of numerical simulation of the flow in the channel of real design of the ITGF setup. At the first stage of computations, the channel was represented as a long hydraulically smooth pipe. In this case, a good agreement of the velocity profile with the analytical solution was obtained. Further, on the basis of the constructed model, the analysis of the factors influencing the velocity profile was carried out. The influence of the Mach number, design features of the setup, and the roughness of the channel walls were considered. It can be concluded that the greatest contribution to the velocity profile change is made by roughness. In this case, for the largest of the considered roughness heights, the velocity profile becomes constant over a length of 45 channel diameters. Since the effect of the real roughness on the velocity profile can only be determined in an experiment on the real ITGF setup, to ensure that the acoustic liner sample is located in the area of the constant velocity profile, it is recommended to increase the length of the test section to the sample up to 60 channel diameters.

## ACKNOWLEDGEMENT

The reported study was funded by RFBR, project number 19-42-590001.

## REFERENCES

- [1] Parrot, T.L., Watson, W.R., Jones, M.G.: Experimental validation of a two-dimensional shear-flow model for determining acoustic impedance, NASA TP-2679, 1987
- [2] Rebel, J., Ronneberger, D.: The effect of shear stress on the propagation and scattering of sound in flow ducts, *Journal of Sound and Vibration*, Vol. 158, No. 3, pp. 469-496, 1992
- [3] Gallman, J.M., Kunza, R.K.: Grazing flow acoustic impedance testing for the NASA AST program, AIAA Paper, No. 2447, 2002
- [4] Elnady, T., Boden, H.: On semi-empirical liner impedance modeling with grazing flow, AIAA Paper, No. 3304, 2003
- [5] Jones, M.G., Parrot, T.L., Watson, W.R.: Comparison of acoustic impedance reduction techniques for locally-reacting liners, AIAA Paper, No. 3306, 2003
- [6] Auregan, Y., Leroux, M., Pagneux, V.: Measurement of liner impedance with flow by an inverse method, AIAA Paper, No. 2838, 2004
- [7] Simonich, J.C., Morin, B.L., Narayanan, S., Patrick, W.P.: Development and qualification of an in-situ grazing flow impedance measurement facility, AIAA Paper, No. 2640, 2006
- [8] Primus, J., Piot, E., Simon, F., Jones, M.G., Watson, W.R.: ONERA-NASA cooperative effort on liner impedance reduction, AIAA Paper, No. 2273, 2013
- [9] Raimo Kabral, Hans Bodén, Tamer Elnady: Determination of liner impedance under high temperature and grazing flow conditions, AIAA Paper, No. 2956, 2014
- [10] Sobolev, A.F., Ostrikov, N.N., Anoshkin, A.N., Palchikovskiy, V.V., Burdakov, R.V., Ipatov, M.S., Ostroumov, M.N., Yakovets, M.A.: Comparison of liner impedance derived from the results of measurements at two different setups using a small number of microphones, *PNRPU Aerospace Engineering Bulletin*, No. 45, p. 59-113, 2016
- [11] Spillere, A.M.N., Medeiros, A.A., Serrano, P.G., Cordioli, J.A.: Cross-validation of a new grazing flow liner test rig using multiple impedance reduction techniques, *The 22-nd International Congress on Sound and Vibration (ICSV-22)*, 12-16 July 2015, Florence, Italy
- [12] Anita Schulz, Chenyang Weng, Friedrich Bake, Lars Enghardt, Dirk Ronneberger: Modeling of liner impedance with grazing shear flow using a new momentum transfer boundary condition, AIAA Paper, No. 3377, 2017
- [13] Serrano, P.G., Spillere, A.M.N., Cordioli, J.A., Murray, P.B., Asltley, R.J.: Comparison of perforated liners impedance experimental techniques, AIAA Paper, No. 3024, 2017
- [14] Ostrikov, N.N., Yakovets, M.A., Ipatov, M.S. Experimental confirmation of an analytical model of the sound propagation in a rectangular duct in the presence of impedance transitions and development of an impedance reduction method based on it, *Acoustical Physics*, Vol. 66, no. 2, p. 105-122, 2020
- [15] Cheng Yang, Penglin Zhang, Stefan Sack, Mats Abom: Low frequency duct noise control using extended tube liners, AIAA Paper, No. 2615, 2020
- [16] Palchikovskiy, V.V., Kustov, O.Yu., Korin, I.A., Cherepanov, I.E., Khramtsov, I.V.: Investigation of acoustic characteristics of liner samples in interferometers with different duct diameter, *PNRPU Aerospace Engineering Bulletin*, No. 51, p. 62-73, 2017
- [17] Watson, W.R., Jones, M.G.: A comparative study of four impedance reduction methodologies using several test liners, AIAA Paper, No. 2274, 2013
- [18] Nikuradse, J.: *Gesetzmässigkeit der turbulenten strömung in glatten rohren*. VDI-Forsch.-Heft 356, VDI-Verl., Berlin, 1932
- [19] Schlichting, H.: *Boundary layer theory*, McGraw-Hill, New York, 1975
- [20] Kirsten, H.: *Experimentelle untersuchung der geschwindigkeitsverteilung bei der turbulenten rohrströmung*, Dissertation, Leipzig, 1927
- [21] Menter, F.R.: Two-equation eddy-viscosity turbulence models for engineering applications, *AIA Journal*, Vol. 32, No. 8, pp. 1598-1605, 1994
- [22] Moody, L.F.: Friction factors for pipe flow, *Transactions of the American Society of Mechanical Engineers*, Vol. 66, pp. 671-681, 1944.



**Vadim Palchikovskiy** is Ph.D. of Engineering Science, researcher of the Laboratory of Noise Generation Mechanisms and Modal Analysis, and Associate Professor of the Perm National Research Polytechnic University. His research area includes acoustic measurements, investigation of characteristics of soundabsorbing structures and materials, numerical methods and programming, numerical simulation of acoustic processes. He presented the main results of scientific research at the international conferences in Moscow, St. Petersburg, Kazan, and Perm.



**Igor Khramtsov** is Ph.D. of Engineering Science, researcher of the Laboratory of Noise Generation Mechanisms and Modal Analysis, and Assistant Professor of the Perm National Research Polytechnic University. His research area includes aeroacoustics, investigation of characteristics of sound-absorbing structures and materials, and acoustic measurements. He presented the main results of scientific research at the international conferences in Moscow, St. Petersburg, Novosibirsk, and Perm.



**Aleksander Kuznetsov** is a student of the Aerospace Faculty of the Perm National Research Polytechnic University. His research area includes duct acoustics, numerical methods and programming, numerical simulation of acoustic processes. He presented the main results of scientific research at the international conferences in Moscow and Perm.



**Victor Pavlogradskiy** is Ph.D. of Engineering Science, Deputy Head of the Department of Rocket and Space Engineering and Power Generating Systems of the Perm National Research Polytechnic University. His research area includes duct acoustics, numerical methods and programming, numerical simulation of acoustic processes. He presented the main results of scientific research at the international conferences in Moscow, St. Petersburg, Kazan, and Perm.